International Journal of Mechanical and Production Engineering Research and Development (IJMPERD)
ISSN (P): 2249-6890; ISSN (E): 2249-8001
Vol. 7, Issue 6, Dec 2017, 21-44

NUMERICAL INVESTIGATIONS FOR THE EFFECT OF COLD AND HOT AIR ON VARIOUS PARAMETERS OF FLOW THROUGH A SUPER SONIC NOZZLE AT HIGHER ALTITUDES

P SRINIVASA RAO[1], CH V K N S N MOORTHY[2] & V SRINIVAS[3]

[1,2]*Institute of Aeronautical Engineering (Autonomous), Hyderabad, Telangana, India*

[3]*GITAM University, Rushikonda, Vishakhapatnam, Andhra Pradesh, India*

ABSTRACT

An ejector system is to be designed in order to pump out the gasses from low pressure to ambient conditions. Ejectors mainly use the principles of fluid dynamics for pumping. They do not consist of any mechanical parts and hence no wear and tear. But consequently the design of the ejectors should be very much precise for the proper and reliable function. In this part of the work, the configuration of a nozzle is calculated from a predefined rocket air ejector configuration. Models are developed and analyzed using numerical simulation software's. Taking the predefined input and boundary conditions, pressure, temperature, Mach number and velocity contours are developed for the analysis to identify the convergence for a flow through nozzle for cold and hot air. Further, Parametric analysis is also carried out by plotting various graphs to understand the corresponding effect.

KEYWORDS: Numerical Simulations, Nozzle Flow & Parametric Analysis

Received: Sep 20, 2017; **Accepted:** Oct 11, 2017; **Published:** Oct 28, 2017; **Paper Id:** IJMPERDDEC20173

Original Article

INTRODUCTION

Most flows occurring in nature and in engineering applications are turbulent. The boundary layer in the earth's atmosphere is turbulent; jet streams in the upper troposphere are turbulent; cumulus clouds are in turbulent motion. The water currents below the surface of the oceans are turbulent. The Gulf Stream is a turbulent wall-jet kind of flow. The photosphere of the sun and the photospheres of similar stars are in turbulent motion; interstellar gas clouds are turbulent; the wake of the earth in the solar wind is presumably a turbulent wake. Turbulence is the feature of fluid flow but not of fluids. Most of the dynamics of turbulence is the same in all fluids, whether they are liquids or gases, if the Reynolds number of the turbulence is large enough; the major characteristics of turbulent flows are not controlled by the molecular properties of the fluid in which the turbulence occurs. Since the equations of motion are nonlinear, each individual flow pattern has certain unique characteristics that are associated with its initial and boundary conditions. No general solution to the Navier-Stokes equations is known; consequently, no general solutions to problems in turbulent flow are available. Since every flow is different, it follows that every turbulent flow is different, even though all turbulent flows have many characteristics in common.

Upper stage rocket motor testing is the most vital, difficult and involves a lot of complexity. The decrease in the atmospheric pressure at higher altitudes affects the performance of launch vehicles. Selection of perfectly suitable fluid dynamic system to pump out the exhaust gases to the ambient at higher altitudes is the most complicated process. As Supersonic exhaust diffusers use the momentum of the exhaust gas to reduce the back

pressure, they can be considered as the most promising alternative for pumping out the exhaust gases in high altitude test facility. In general, two types of supersonic exhaust diffusers with zero secondary flow injection are used in high test facilities; one being the constant area duct type or the Straight Cylindrical Exhaust Diffuser and the other one is the variable area duct or the Second Throat supersonic Exhaust Diffuser.

Most of the studies carried out the flow through the convergent divergent nozzle by using a finite volume rewarding code with energy equation, K epsilon viscous model [1]. The increase in the velocity, and decrease in the pressure and temperature are observed all through the Nozzle. Convergent divergent nozzle can show better performance than bell nozzle, dual bell nozzle and expandable nozzles [2]. Mach number initially decreases and then increases with the increase in the divergence angle [3] for the supersonic flow in conical nozzle for Mach number 3 at constant throat and inlet diameters. It is also observed that the flow to be super-sonic at exit, decrease in the pressure, increase in the velocity and increase in radial velocity from inlet to outlet is identified during the analysis of dual bell rocket nozzle. Researches published that the best nozzle performance is obtained for nozzle with 11degrees angle of divergence for both air and gas [4, 5]. So the nozzle of 11degrees is the best nozzle to accelerate the flows up to supersonic mach speeds. During simulation analysis on a convergent divergent nozzle k- model receives higher average values of Mach number in contrast to k-ω model [6]. Further fluid properties are largely dependent on the cross section of the nozzle which greatly affects the fluid flow [7]. Computational Fluid Dynamic (CFD) simulation results are almost identical to those obtained theoretically [8, 9]. Recent publications report that the continuous increase of nozzle area ratio of satellite launch vehicles for getting the optimum expansion during the mission will contribute up to 20 % of thrust augmentation at low altitudes [10]. When the Flow is from converging nozzle to suddenly expanded circular duct of larger cross-sectional area than that of nozzle exit area, it is found that as the NPR increases, the effect on base pressure is marginal for NPRs up to 2.5; however, at NPR 3 there is a sudden decrease in the base pressure [11] and the viscosity accounts to loss in momentum [12]. It is found that the nozzle-rotor interaction losses can be decreased by selecting appropriate length of axial clearance [13-15]. The CFD model fails to converge if the grid quality is poor and the complexity of the flow near the stagnation region is high [17, 18]. The concept of design of the air ejector is presented in detail with various correlations as mentioned in [19]. The compressible fluid flow computational analysis methodology is presented in detail with the turbulence modeling and numerical analysis in [20].

PROBLEM BACKGROUND

An ejector system is designed for the connect pipe facility. The Connect pipe test facility was preliminarily planned with 7.1 kg/s. of Air ejector to simulate 20km altitude condition. During main design phase, with the available theoretical models it was calculated that around 15 kg/s of air is required to simulate 20km altitude.

The methodology in calculating the nozzle physical parameters using the correlations mentioned from equations (1) to (5) is described in [19].

Plenum chamber- diffuser-ejector systems are required for high altitude rocket motor test facilities. A 1D Fluid dynamic model was developed to pump out the rocket exhaust from 50 mbar at 20 km altitude to atmospheric condition of 1050mbar. The developed model of a convergent divergent nozzle with diffuser has 76.5mm inlet and exit diameters with 23.5mm throat diameter which has a length of 325mm with 30^o and 7^o convergence and divergence angles. Further the diffuser with 692mm is connected at the end of the nozzle.

By applying the following correlations to the dimensions of the nozzle the results of various physical parameters are calculated and tabulated in table 1.

$$A_e/A^* = \left(\frac{\gamma+1}{2}\right)^{\frac{-(\gamma+1)}{2(\gamma-1)}} \frac{\left(1+\frac{\gamma-1}{2}M_e^{\,2}\right)^{\frac{-(\gamma+1)}{2(\gamma-1)}}}{M_e} \quad (1)$$

$$P_e/P_t = \left(1+\frac{\gamma-1}{2}M_e^{\,2}\right)^{\frac{-\gamma}{\gamma-1}} \quad (2)$$

$$T_e/T_t = \left(1+\frac{\gamma-1}{2}M_e^{\,2}\right)^{-1} \quad (3)$$

$$\dot{m} = \left(\frac{A^*P_t}{\sqrt{T_t}}\right)\sqrt{\frac{\gamma}{R}}\left(\frac{\gamma+1}{2}\right)^{\frac{-(\gamma+1)}{2(\gamma-1)}} \quad (4)$$

$$V_e = M_e\sqrt{\gamma R T_e} \quad (5)$$

Table 1: Results of Nozzle Parameters

Nozzle Parameters	Result Values
ṁ (Kg/s)	15
P_e (Pa)	8040Pa
Me	4
To (K)	300
P_o(bar)	7.59
T_e (K)	71.43
Ae/A*	10.719
De (m)	0.184
D* (m)	0.133

METHODOLOGY

The analysis is carried out both with the mathematical and the Computational Fluid Dynamics simulation.

Methodology for Numerical Analysis

The flow of the fluid through air ejector is always more unsteady and turbulent which further makes the design more complicated. For all turbulent flows the governing equations are the unsteady Navier Stokes equations. But those equations are very much difficult to solve. The following are the governing equations in tensor notation for understanding the basic nature of the equation.

$$\frac{\partial \rho u_i}{\partial t} + \frac{\partial(\rho u_i u_j)}{\partial x_j} = -\frac{\partial(p)}{\partial x_i} + \frac{\partial}{\partial x_j}\left(\mu\left[\frac{\partial(u_i)}{\partial x_j} + \frac{\partial(u_j)}{\partial x_i}\right]\right) - \frac{\partial}{\partial x_i}\left(\frac{2}{3}\mu\frac{\partial(u_k)}{\partial x_k}\right) + S_i \quad (1)$$

Energy equation is given by

$$\frac{\partial \rho \epsilon}{\partial t} + \frac{\partial (\rho u_j e)}{\partial x_j} = -p\frac{\partial (u_j)}{\partial x_j} + \frac{\partial}{\partial x_j}\left(k\frac{\partial (T)}{\partial x_j}\right) + \emptyset + S_i \tag{2}$$

Where,

$$\emptyset = \left(\mu\frac{\partial (u_i)}{\partial x_j}\left[\frac{\partial (u_i)}{\partial x_j} + \frac{\partial (u_j)}{\partial x_i}\right]\right) - \left(\frac{2}{3}\mu(\frac{\partial (u_k)}{\partial x_k})^2\right) \tag{3}$$

The main disadvantage in solving N-S equations is computing. This is due to the reason that to represent even very small scale of velocity and pressure fluctuations using N-S equations temporal resolution is required as the N-S equations are spatial fineness equations. Further the accuracy and resolution of the scheme reduces due to the increase in accumulative rounding off value errors because of the increase in grid points to achieve fine meshes. Hence more accurate schemes are required to achieve the solutions of turbulence models with highest resolution. One such numerical scheme which can effectively solve the turbulence problems is Reynolds Averaged Navier-Stokes (RANS) equations.

Reynolds Averaged Navier-Stokes (RANS) Equations

The transport equations should be modified by introducing the components with averaged and fluctuating components for solving the turbulent models. RANS are the equations of the motion of the fluid flow with time – averaged equations. If flow turbulence properties are known then suitable approximations can be made and high resolution solutions to the N-S equations can be achieved by solving the RANS equations. The RANS equations in tensor notation are described below

$$\rho\frac{\partial \overline{u_i}}{\partial t} + \rho\frac{\partial (\overline{u_i u_j})}{\partial x_j} = \rho\overline{f_i} + \frac{\partial}{\partial x_j}\left(-\overline{p}\delta_{ij} + 2\mu\overline{S_{ij}} - \rho\overline{u_i' u_j'}\right) \tag{4}$$

Where $\overline{S_{ij}} = \frac{\partial (\overline{u_i})}{\partial x_j} + \frac{\partial (\overline{u_j})}{\partial x_i}$ is the mean rate of strain tensor.

The problems of physical engineering which involve high turbulence when modelled based on RANS equations are also called statistical turbulence models because the method strongly involves statistical averaging procedure. Consequently, the computational effort to solve RANS equations is very less when compared to other schemes.

Governing equations for turbulence models

As discussed in the earlier articles, due to the involvement of more unknown parameters in the modelling of turbulent problems, the accuracy of the model becomes very much difficult and leads to erroneous results. Hence it is required to develop a numerical procedure to close or converge the system of equations. One such two equations category turbulence model is K-epsilon model.

K-Epsilon Models

In this model the velocity of the turbulent flow and the length scales are independently calculated using two different equations. The basic model is the standard k-epsilon model.

Standard k-ε Model

The velocity of the turbulence can be calculated by forming a model for the corresponding kinetic energy using the following equation

$$\frac{\partial(\rho k)}{\partial t}+\frac{\partial(\rho k u_i)}{\partial x_i}=\frac{\partial}{\partial x_j}\left[\left(\mu+\frac{\mu_t}{\sigma_k}\right)\frac{\partial(k)}{\partial x_j}+P_k+P_b-\rho\varepsilon-Y_M+S_k\right] \quad (5)$$

The length scale is represented by ε which is the rate of dissipation and can be calculated from the equation

$$\frac{\partial(\rho \epsilon)}{\partial t}+\frac{\partial(\rho \epsilon u_i)}{\partial x_i}=\frac{\partial}{\partial x_j}\left[\left(\mu+\frac{\mu_t}{\sigma_\epsilon}\right)\frac{\partial(\epsilon)}{\partial x_j}+C_{1\epsilon}\frac{\epsilon}{k}(P_k+C_{3\epsilon}P_b)-C_{2\epsilon}\rho\frac{\varepsilon^2}{k}+S_\epsilon\right] \quad (6)$$

Where P_k represents the turbulence kinetic energy due to the mean velocity gradients, P_b represents the turbulence kinetic energy due to buoyancy and Y_M represents the contribution of the fluctuating dilatation in compressible turbulence to the overall dissipation rate.

RESULTS AND DISCUSSIONS

2D Axis-symmetric model has been considered for single stage ejector system CFD simulation. Plenum chamber has been simplified to a small volume region for sake of convergence. A large volume dome atmosphere has been modeled at the exit of mixing chamber to simulate the atmosphere at 1 bar. The geometric model has been prepared in AutoCAD then meshing, Boundary condition definitions, solver settling and solution has been carried out using ANSYS Cfx. To study the performance of the ejector, the cell pressure and diffuser pressure recovery are to be recorded.

Effect of Exit Pressure on Pressure for Cold Fluid during Flow

The inlet temperature of fluid is taken as 300K.

By varying the exit pressure of fluid in a CD nozzle the pressure contours are developed and the pressures are approximately identified by using the colour coding along the pressure scale. Accurate results can be obtained by using probe at a specified location.

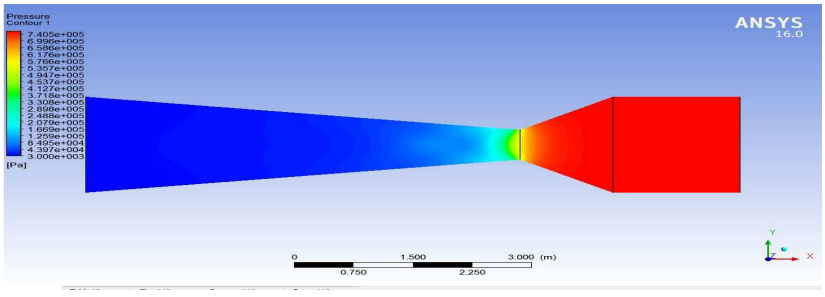

Figure 1: Pressure Contour at 30mbar Exit Pressure

Pressure contour has been developed at 30mbar exit pressure. The pressure in the CD nozzle at throat reached to 4.992 bar at the throat and reduced to 3000 mbar at the exit.

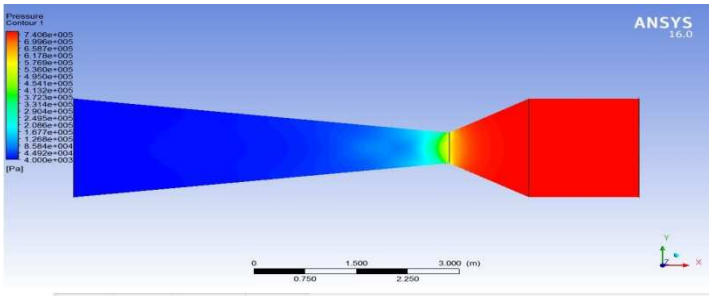

Figure 2: Pressure Contour at 40mbar Exit Pressure

Pressure contour has been developed at 40mbar exit pressure. The pressure at the throat has reached to 4.80 bar and dropped to 4000 mbar at the exit.

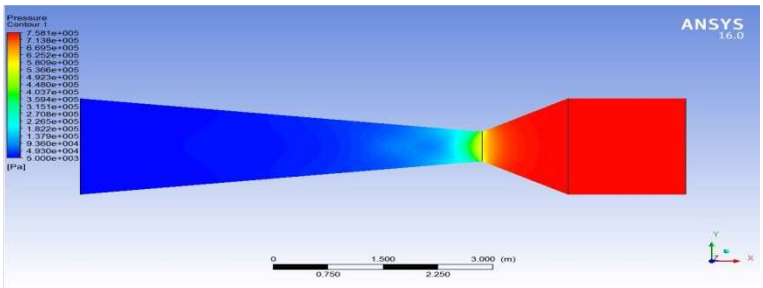

Figure 3: Pressure Contour at 50mbar Exit Pressure

Pressure contour has been developed at 50mbar exit pressure. The pressure at the throat is 4.589 bar and then due to divergent portion it has been drastically reduced to 5000 mbar. Variation of pressure for cold fluid at various exit pressures are tabulated in table 2.

Table 2: Pressure at Inlet, Throat and Exit at Various Exit Pressures

Exit Pressures	30mbar	40mbar	50mbar
Inlet pressure (bar)	7.405	7.5738	7.5738
Throat pressure (bar)	4.992	4.8084	4.5859
Exit pressure (bar)	0.03	0.0482	0.0516

The results are plotted on graph for understanding parametric effect shown in Figure.4

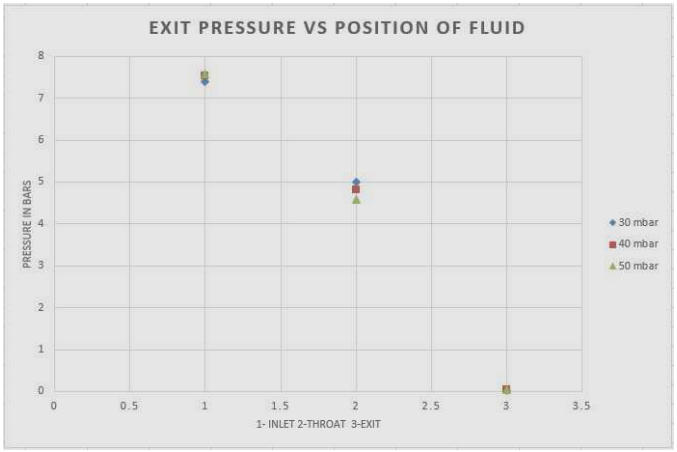

Figure 4: Variation of Inlet, Throat and Exit Pressures Due to Change in Outlet Pressure of a CD Nozzle

From figure 4 it is evident that the inlet pressure increases with decrease in exit pressure of the CD nozzle. Also, it

is observed that the throat pressure decreases with increase in exit pressure of the nozzle.

Effect of Exit Pressure on Mach for Cold Fluid during Flow

The inlet temperature of fluid is taken as 300K. By varying the exit pressure of fluid in a CD nozzle the mach contours are developed and the mach values are approximately identified by using the colour coding along the mach scale.

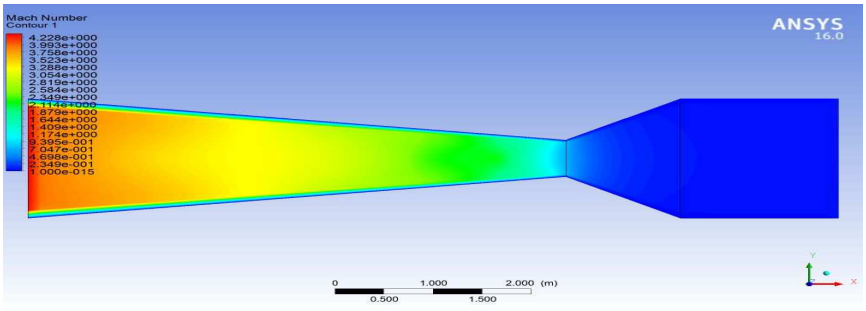

Figure 5: Mach Contour at 30mbar Exit Pressure

Mach contour has been developed at 30mbar exit pressure. Mach number at throat is 0.707 and then it has been increased to 4.228 at the exit of the CD nozzle due to the divergent portion which results in increase in velocity.

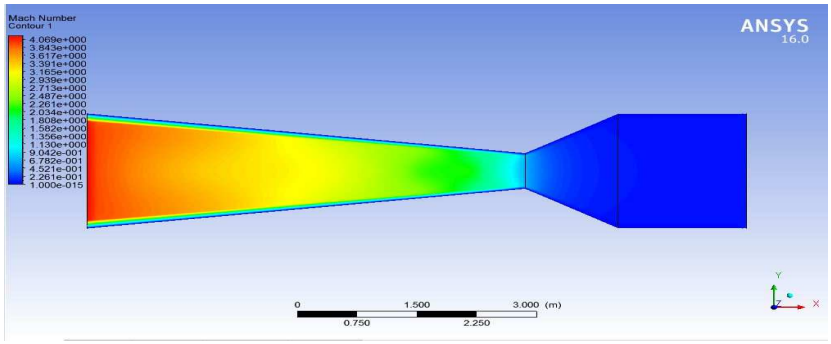

Figure 6: Mach Contour at 40mbar Exit Pressure

Mach contour has been developed at 40mbar exit pressure. Mach number at throat is observed to be 0.773 and it has been increased to 4.162 at the exit of CD nozzle.

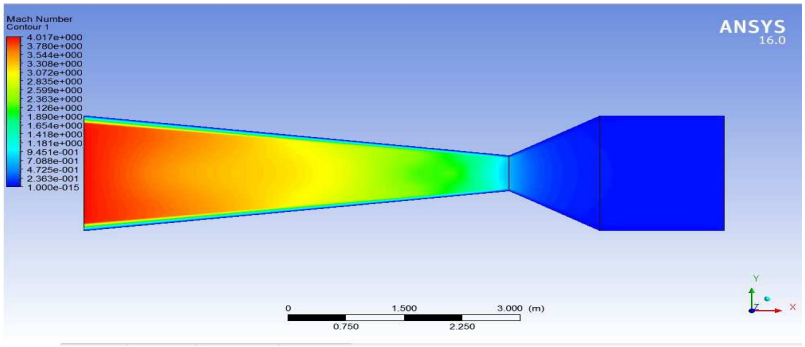

Figure 7: Mach Contour at 50mbar Exit Pressure

Mach contour has been developed at 50mbar exit pressure. Mach number at throat is 0.676 and it is observed that is has risen up to 4.01 by the time it reaches the exit of the CD nozzle.

By considering all the values of mach numbers with respect to exit pressures, the table 3 is plotted for further analysis. Variation of mach number for cold fluid at various exit pressures are tabulated in table 2

Table 3: Mach number at Inlet, Throat and Exit at Various Exit Pressures

Exit Pressures	30mbar	40mbar	50mbar
Inlet Mach	0.0548	0.05552	0.05553
Throat Mach	0.7076	0.7728	0.676085
Exit Mach	4.228	4.1622	4.0111

The results are plotted on graph for understanding parametric effect shown in Figure.8

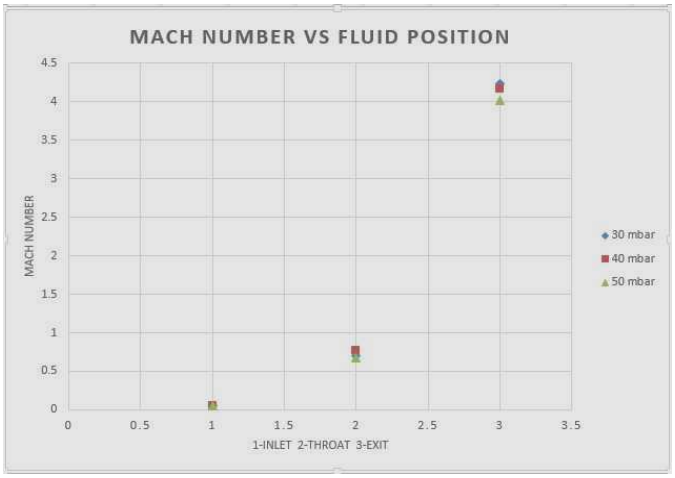

Figure 8: Variation of Mach number at Inlet, Throat and Exit of CD Nozzle Due to Change in Exit Pressure

From figure 8 it is evident that the mach number increases with decrease in exit pressure of the CD nozzle.

Effect of Exit Pressure on Temperature for Cold Fluid during Flow

The inlet temperature of fluid is taken as 300K. By varying the exit pressure of fluid in a CD nozzle the temperature contours are developed and the temperatures are approximately identified by using the colour coding along the temperature scale.

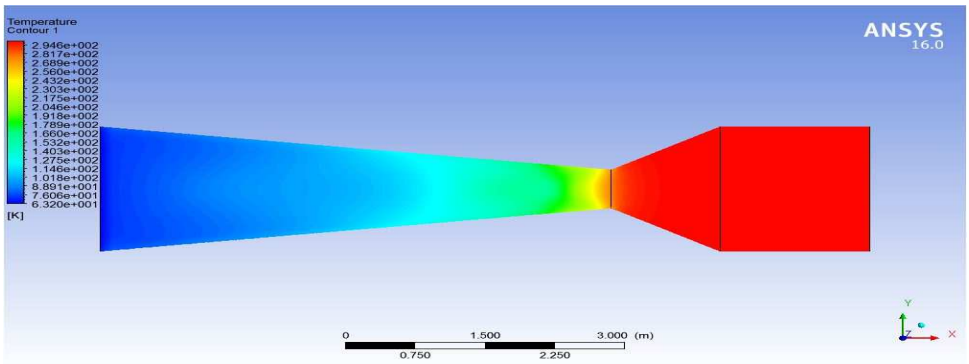

Figure 9: Temperature Contour at 30mbar Exit Pressure

Temperature contour has been developed at 30mbar exit pressure. Temperature at throat is found to be 269.96 K and it is greatly reduced up to 63.2 K at the exit of the CD nozzle.

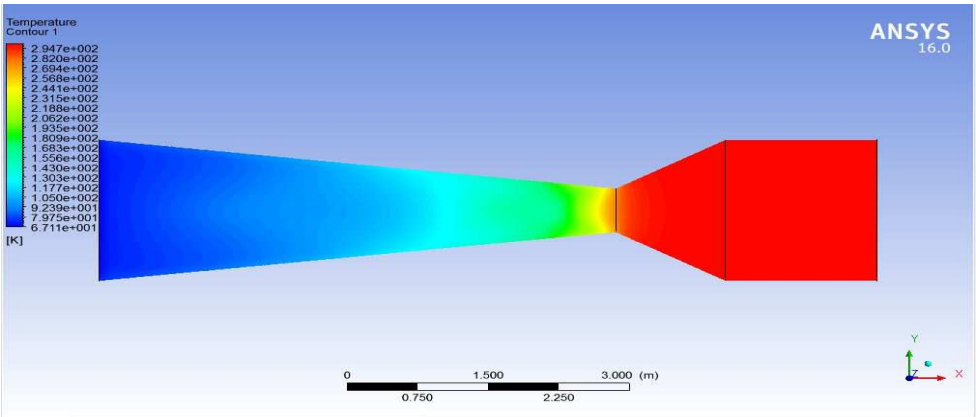

Figure 10: Temperature Contour at 40mbar Exit Pressure

Temperature contour has been developed at 40mbar exit pressure. The temperature at throat is 267.86 K and it has been reduced to 67.19 K by the moment it reaches the exit of the CD nozzle.

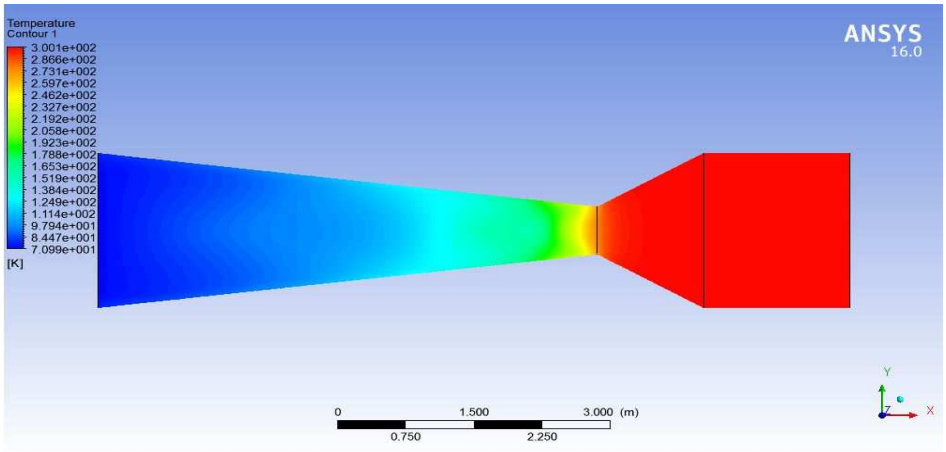

Figure 11: Temperature Contour at 50mbar Exit Pressure

Temperature contour has been developed at 50mbar exit pressure. The temperature at throat is 274.88 K and it has been reduced to 71.13 K by the moment it reaches the exit of the CD nozzle.

The table 4 is generated by taking all the parameters of pressure and temperature in to consideration for better analysis. Variations of temperature number for cold fluid at various exit pressures are tabulated:

Table 4: Temperature at Inlet, Throat and Exit at Various Exit Pressures

Exit Pressures	30mbar	40mbar	50mbar
Inlet Temperature (K)	300	300	300
Throat Temperature (K)	269.968	267.861	274.883
Exit Temperature (K)	63.2	67.1993	71.1339

The results are plotted on graph for understanding parametric effect shown in Figure.12

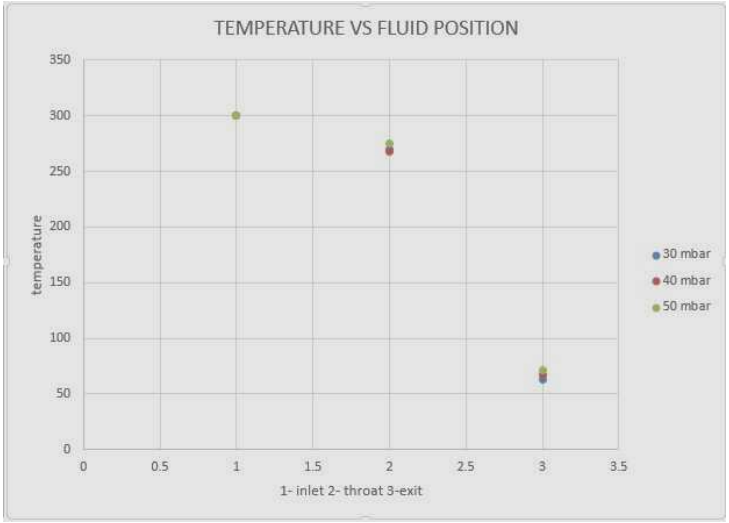

Figure 12: Variation of Inlet, Throat and Exit Temperatures of a CD Nozzle with Change in Exit Pressure

From figure 12 it is evident that the temperature increases with increase in exit pressure of the CD nozzle due to the collision of fluid molecules under the effect of back pressure.

Effect of Exit Pressure on Pressure for Hot Fluid during Flow

The inlet temperature of fluid is taken as 1250K.

By varying the exit pressure of fluid in a CD nozzle the pressure contours are developed and the pressures are approximately identified by using the colour coding along the pressure scale.

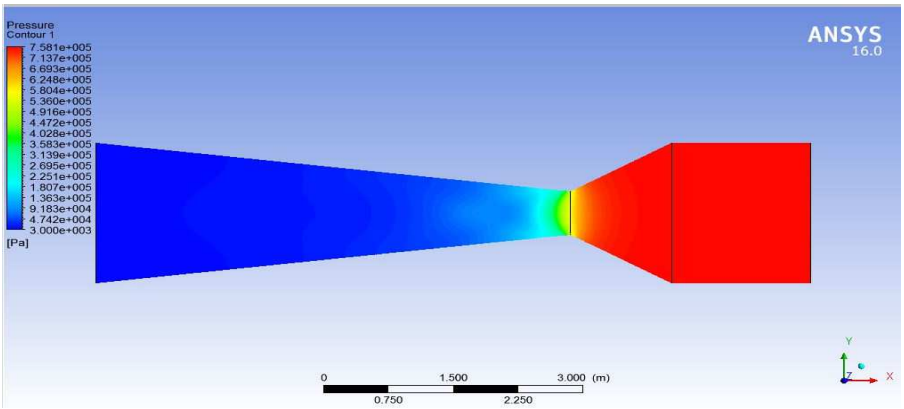

Figure 13: Pressure Contour at 30mbar Exit Pressure

Pressure contour has been developed at 30mbar exit pressure. The pressure at throat is observed to be 5.585 bars and it has been reduced to 30 mbar due to the effect of divergent portion.

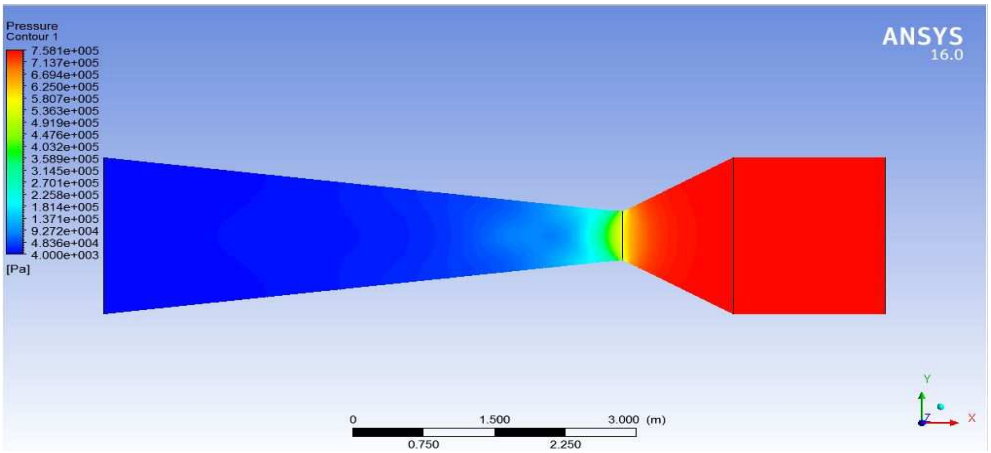

Figure 14: Pressure Contour at 40mbar Exit Pressure

Pressure contour has been developed at 40mbar exit pressure. The pressure at throat is observed to be 5.585 bars and it has been reduced to 44.6 mbar.

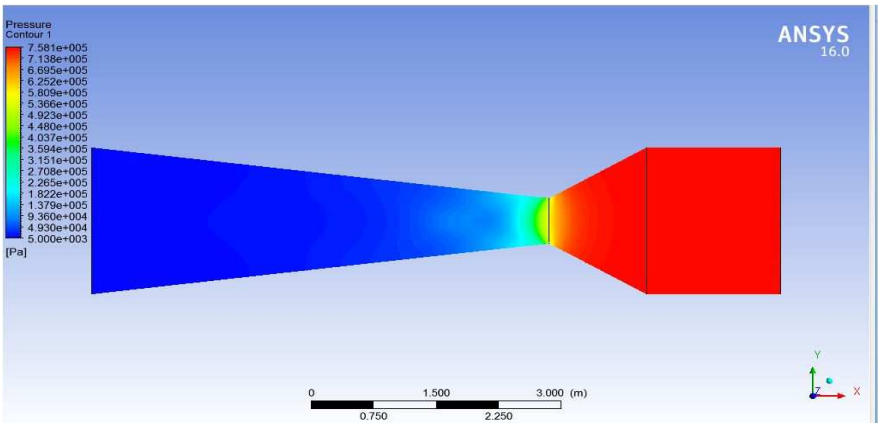

Figure 15: Pressure Contour at 50mbar Exit Pressure

Pressure contour has been developed at 50mbar exit pressure. The pressure at throat is observed to be 5.585 bars and it has been reduced to 51.63 mbar. The table 5 is generated by taking all the parameters of pressure in to consideration for better analysis. Variation of pressure for hot fluid at various exit pressures are shown in table 4

Table 5: Pressure at Inlet, Throat and Exit at Various Exit Pressures

Exit Pressures	30mbar	40mbar	50mbar
Inlet pressure (bar)	7.573	7.5738	7.5738
Throat pressure (bar)	5.5859	5.5859	5.5859
Exit pressure (bar)	0.0446	0.04809	0.05163

The results are plotted on graph for understanding parametric effect shown in Fig.16. From figure 5.16 it is evident that the inlet pressure increases with decrease in exit pressure of the CD nozzle. Also, it is observed that the throat pressure decreases with increase in exit pressure of the nozzle.

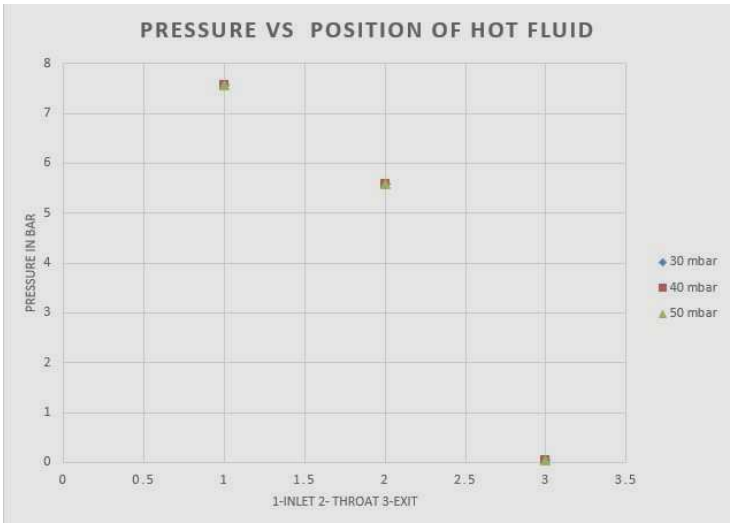

Figure 16: Variation of Pressure at Inlet, Throat and Exit of a CD Nozzle with Change in Exit Pressure for a hot fluid

Effect of Exit Pressure on Mach for Hot Fluid during Flow

The inlet temperature of fluid is taken as 1250K. By varying the exit pressure of fluid in a CD nozzle the mach contours are developed and the mach values are approximately identified by using the colour coding along the mach scale.

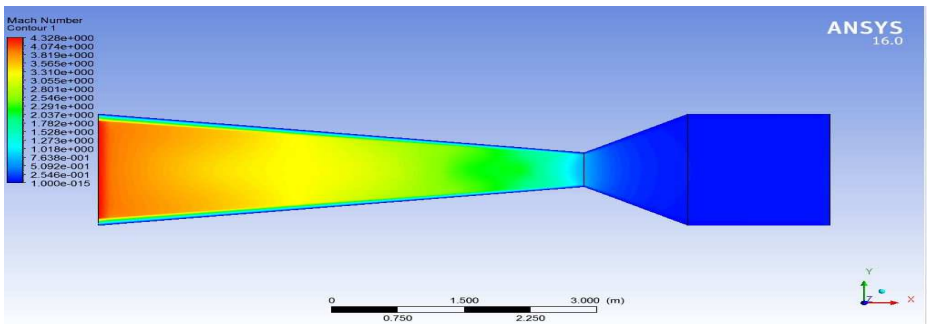

Figure 17: Mach Contour at 30mbar Exit Pressure

Mach contour has been developed at 30mbar exit pressure. Mach number at throat is observed to be 0.676 and it has been increased to 4.323 at the exit of CD nozzle.

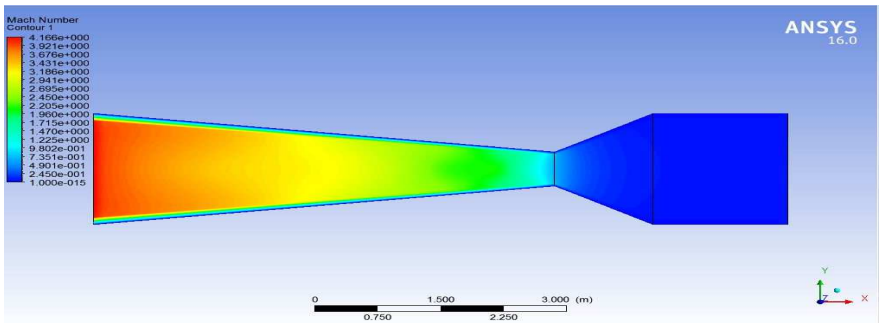

Figure 18: Mach Contour at 40mbar Exit Pressure

Mach contour has been developed at 40mbar exit pressure. Mach number at throat is observed to be 0.676 and it has been increased to 4.16 at the exit of CD nozzle.

Mach contour has been developed at 50mbar exit pressure. Mach number at throat is observed to be 0.676 and it has been increased to 4.01 at the exit of CD nozzle.

The table 4 is generated by taking all the parameters of pressure and mach number in to consideration for better analysis. Variation of mach number for hot fluid at various exit pressures are tabulated in table 6.

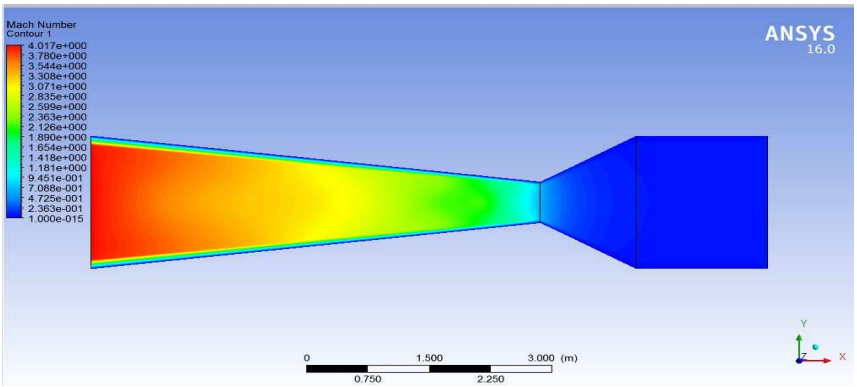

Figure 19: Mach Contour at 50mbar Exit Pressure

Table 6: Mach number at Inlet, Throat and Exit at Various Exit Pressures

Exit Pressures	30mbar	40mbar	50mbar
Inlet Mach	0.05523	0.055523	0.55523
Throat Mach	0.67609	0.67609	0.67609
Exit Mach	4.3236	4.1606	4.01116

The results are plotted on graph for understanding parametric effect as shown in Fig.20

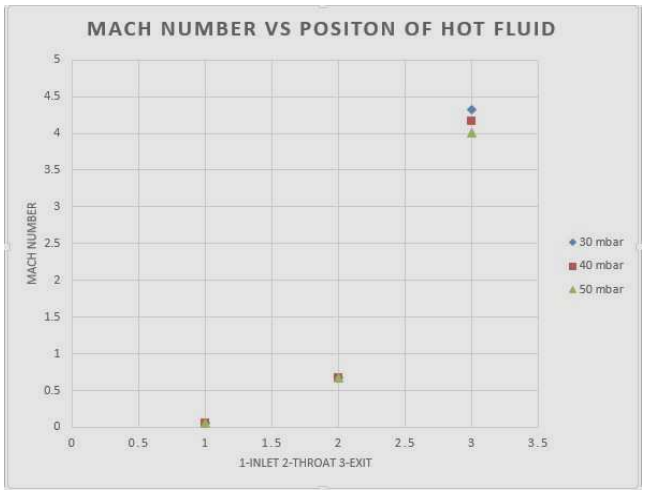

Figure 20 Variation of Mach number at Inlet, Throat and Exit of a CD Nozzle with Change in Exit Pressure for a Hot Fluid

From figure 20 it is evident that the Mach number increases with decrease in exit pressure of the CD nozzle and remained constant at the throat.

Effect of Exit Pressure on Temperature for Hot Fluid during Flow

The inlet temperature of fluid is taken as 1250K. By varying the exit pressure of fluid in a CD nozzle the temperature contours are developed and the temperatures are approximately identified by using the colour coding along the

temperature scale.

Temperature contour has been developed at 30mbar exit pressure. The temperature at throat is 1145.35 K and it has been reduced to 263.81 K by the moment it reaches the exit of the CD nozzle.

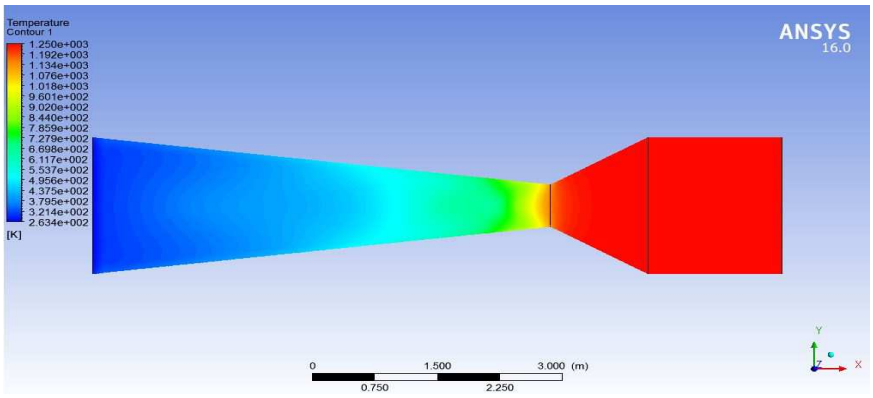

Figure 21: Temperature Contour at 30mbar Exit Pressure

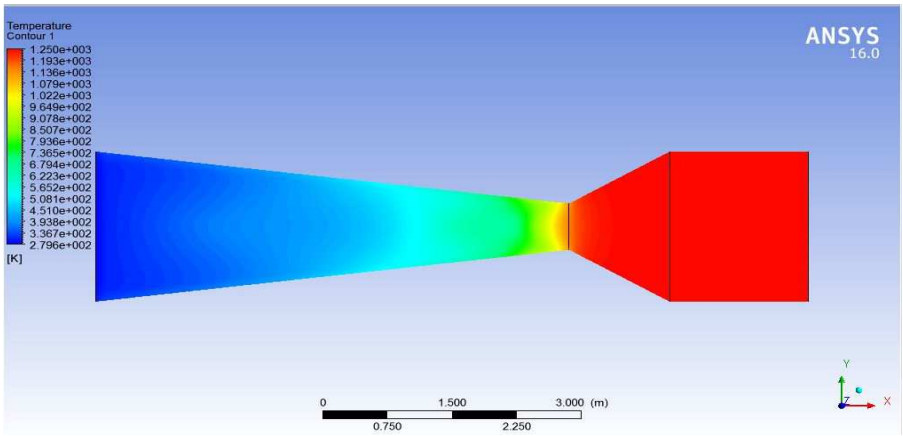

Figure 22: Temperature Contour at 40mbar Exit Pressure

Temperature contour has been developed at 40mbar exit pressure. The temperature at throat is 1145.35 K and it has been reduced to 269.96 K by the moment it reaches the exit of the CD nozzle.

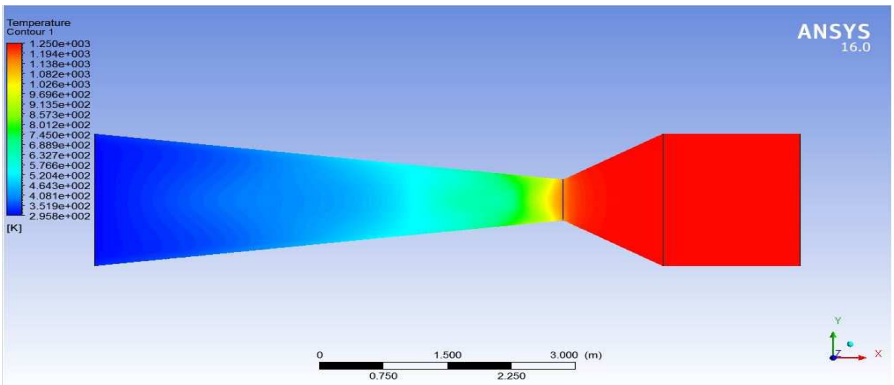

Figure 23: Temperature Contour at 50mbar Exit Pressure

Temperature contour has been developed at 50mbar exit pressure. The temperature at throat is 1145.35 K and it has been reduced to 296.39 K by the moment it reaches the exit of the CD nozzle.

The table 7 is generated by taking all the parameters of pressure and temperature in to consideration for better analysis. Variation of temperature number for hot fluid at various exit pressures are tabulated in table 6.

Table 7: Temperature at Inlet, Throat and Exit at Various Exit Pressures

Exit Pressures	30mbar	40mbar	50mbar
Inlet Temperature (K)	1250	1250	1250
Throat Temperature (K)	1145.35	1145.35	1145.35
Exit Temperature (K)	263.811	269.968	296.395

The results are plotted on graph for understanding parametric effect shown in Figure.24

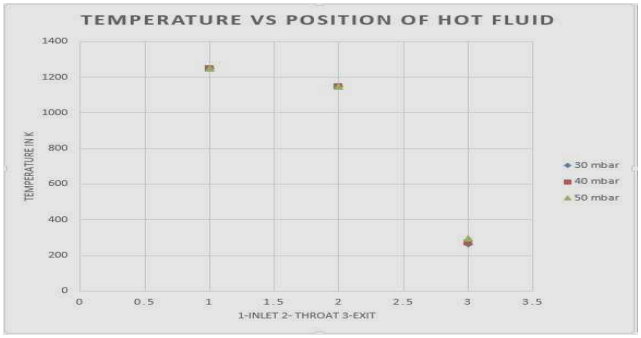

Figure 24: Variation of Temperature at Inlet, Throat and Exit of a CD Nozzle with Change in Exit Pressure for a hot Fluid

From figure 24 it is evident that the temperature increases with increase in exit pressure of the CD nozzle due to the collision of fluid molecules under the effect of back pressure.

Effect of Temperature on the Pressure for Exit Pressure of 50mbar during Flow

The exit pressure of the fluid is taken as 50mbar with the inlet temperatures of 300K and 1250K. The contours are developed as shown in the figures Fig.3, and Fig.15. Variation of pressures with inlet temperatures are tabulated in table 8

Table 8: Pressure at Inlet, Throat and Exit at Different Inlet Fluid Temperatures at 50mbar

	Inlet Pressure (bar)	Throat Pressure (bar)	Exit Pressure (bar)
At inlet temperature of 300K	7.5738	4.5859	0.516
At inlet temperature of 1250K	7.5738	5.5839	0.05163

The results are plotted on graph for understanding parametric effect shown in Figure.25

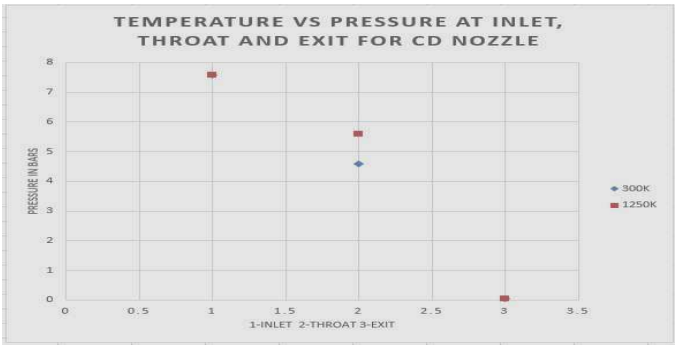

Figure 25: Variation of Pressure at Inlet, Throat and Exit of a CD Nozzle with Change in Temperature of Inlet Fluid at 50 mbar Exit Pressure

From figure 25 it is concluded that the inlet and exit pressures remained same, but due to raise in temperature of inlet fluid temperature throat pressure is increased.

Effect of Temperature on the Mach for Exit Pressure of 50mbar during Flow

The exit pressure of the fluid is taken as 50mbar with the inlet temperatures of 300K and 1250K. The contours are developed as shown in the figures Figure 7 and Figure.19. Variation of mach numbers with inlet temperatures are tabulated in table 9.

Table 9: Mach numbers at Inlet, Throat and Exit at Different Inlet Temperatures at 50mbar

	Inlet Mach	Throat Mach	Exit Mach
At inlet temperature of 300K	0.05553	0.676085	4.0111
At inlet temperature of 1250K	0.05523	0.67609	4.01116

The results are plotted on graph for understanding parametric effect shown in Fig.26

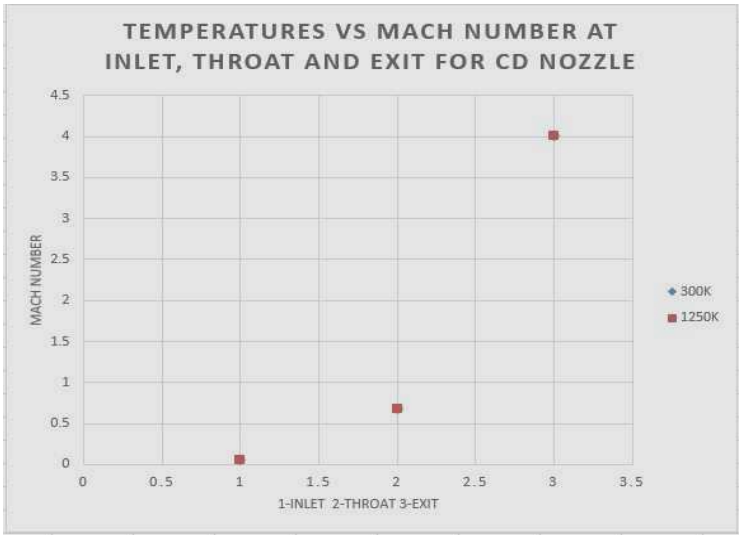

Figure 26: Variation of Mach number at Inlet, Throat and Exit with Change in Temperature of Inlet Fluid at 50 mbar exit pressure

From the figure 26 it is well observed that there is no appreciable change in mach number with raise in fluid inlet temperature.

Effect of Temperature on the Temperatures for Exit Pressure of 50mbar during Flow

The exit pressure of the fluid is taken as 50mbar with the inlet temperatures of 300K and 1250K. The contours are developed as shown in the figures Fig.11, and Fig.23. Variation of temperatures with inlet temperatures are tabulated in table 10.

Table 10: Temperature at Inlet, Throat and Exit at Different Inlet Temperatures at 50mbar

	Inlet Temperature(K)	Throat Temperature(K)	Exit Temperature(K)
At inlet temperature of 300K	300	274.883	71.1339
At inlet temperature of 1250K	1250	1145.35	296.395

The results are plotted on graph for understanding parametric effect shown in Fig.27. From figure 27 it is concluded that temperature of the inlet fluid reduces to a greater extent. The rate of decrease of temperature is directly

proportional to the inlet fluid temperature.

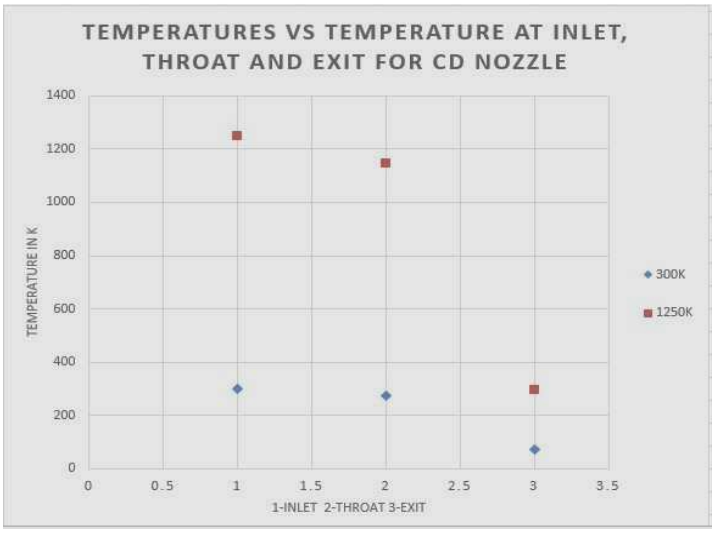

Figure 27: Variation of Temperature at Inlet, Throat and Exit in a CD Nozzle with Change in Inlet Temperature of Fluid at 50 mbar Exit Pressure

Effect of Temperature on the Pressure for Exit Pressure of 40mbar during Flow

The exit pressure of the fluid is taken as 40mbar with the inlet temperatures of 300K and 1250K. The contours are developed as shown in the figures Fig.2 and Fig.14. Variation of pressures with inlet temperatures are tabulated in table 11.

Table 11: Pressure at Inlet, Throat and Exit at Different Inlet Temperatures at 40mbar

	Inlet Pressure(bar)	Throat Pressure(bar)	Exit Pressure(bar)
At inlet temperature of 300K	7.5738	4.80841	0.0482
At inlet temperature of 1250K	7.5738	5.5859	0.04835

The results are plotted on graph for understanding parametric effect shown in Fig.28

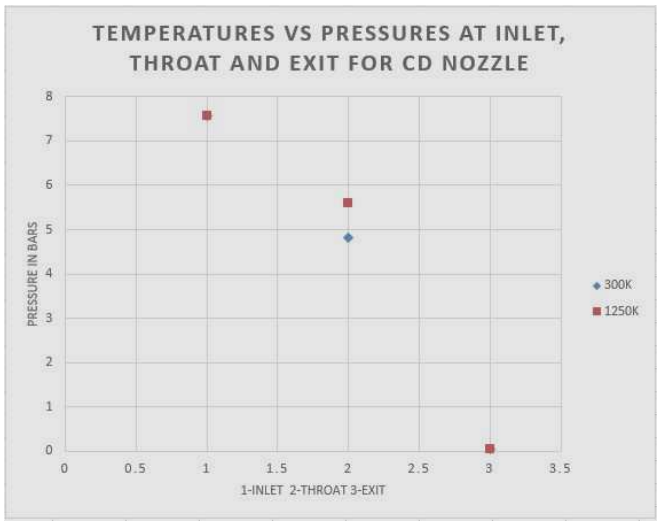

Figure 28: Variation of Pressure at Inlet, Throat and Exit of a CD Nozzle with Change in Inlet Temperature of Fluid at 40 mbar Exit Pressure

From figure 28 it is observed that the inlet and exit pressures does not differ much in their magnitude but, the throat pressure is higher for the fluid with higher inlet fluid temperature.

Effect of Temperature on the Mach for Exit Pressure of 40mbar during Flow

The exit pressure of the fluid is taken as 40mbar with the inlet temperatures of 300K and 1250K. The contours are developed as shown in the figures Fig.6, and Fig.18.

Variations of mach numbers with inlet temperatures are tabulated in table 12

Table 12: Mach numbers at Inlet, Throat and Exit at Different Inlet Temperatures at 40mbar

	Inlet Mach	Throat Mach	Exit Mach
At inlet temperature of 300K	0.05552	0.7728	4.1622
At inlet temperature of 1250K	0.05523	0.77609	4.1606

The results are plotted on graph for understanding parametric effect shown in Fig.29

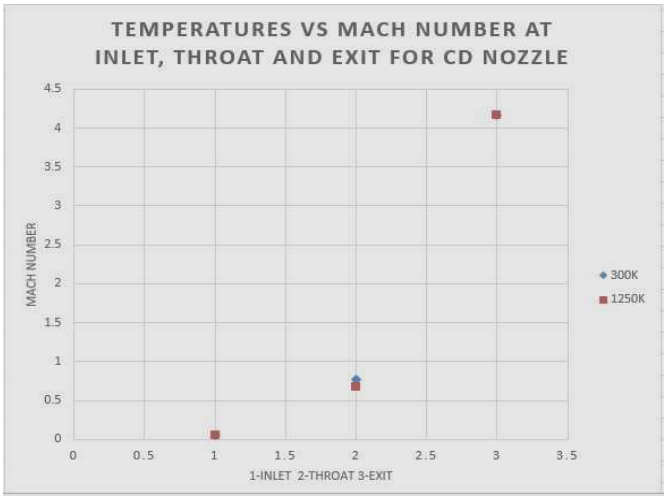

Figure 29: Variation of Mach number at Inlet, Throat and Exit of a CD Nozzle with Change in Inlet Temperature of the Fluid at 40 mbar Exit Pressure

From the figure 29 it is well observed that there is no appreciable change in mach number with raise in fluid inlet temperature.

Effect of Temperature on the Temperatures for Exit Pressure of 40mbar during Flow

The exit pressure of the fluid is taken as 40mbar with the inlet temperatures of 300K and 1250K. The contours are developed as shown in the figures Fig.10, and Fig.22. Variations of temperatures with inlet temperatures are tabulated in table 13.

Table 13: Temperature at Inlet, Throat and Exit at Different Inlet Temperatures at 40mbar

	Inlet Temperature(K)	Throat Temperature(K)	Exit Temperature(K)
At inlet temperature of 300K	300	267.861	67.1993
At inlet temperature of 1250K	1250	1145.35	296.968

The results are plotted on graph for understanding parametric effect shown in Fig.30. From figure 30 it is concluded that temperature of the inlet fluid reduces to a greater extent. The rate of decrease of temperature is directly proportional to the inlet fluid temperature.

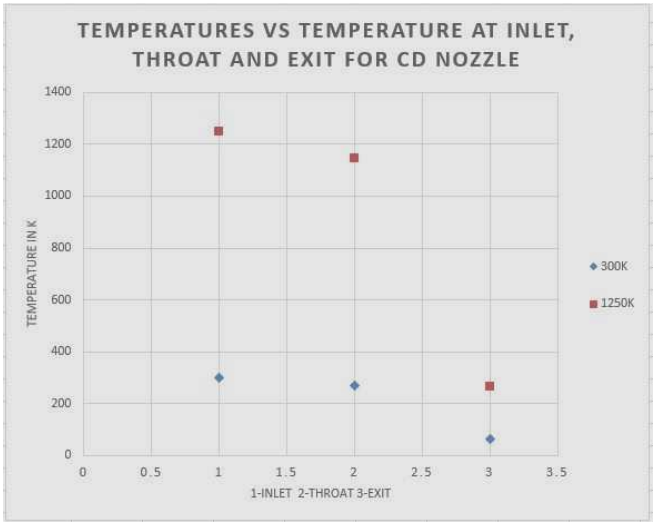

Figure 30: Variation of Temperature at Inlet, Throat and Exit of a CD Nozzle with Change in Inlet Temperature of the Fluid at 40 mbar Exit Pressure

Effect of Temperature on the Pressure for Exit Pressure of 30mbar during Flow

The exit pressure of the fluid is taken as 30mbar with the inlet temperatures of 300K and 1250K. The contours are developed as shown in the figures Fig.1, and Fig.15. Variations of pressures with inlet temperatures are tabulated:

Table 14: Pressure at Inlet, Throat and Exit at Different Inlet Temperatures at 30mbar

	Inlet Pressure(bar)	Throat Pressure(bar)	Exit Pressure(bar)
At inlet temperature of 300K	7.405	4.992	0.03
At inlet temperature of 1250K	7.573	5.5859	0.0346

The results are plotted on graph for understanding parametric effect shown in Fig.31

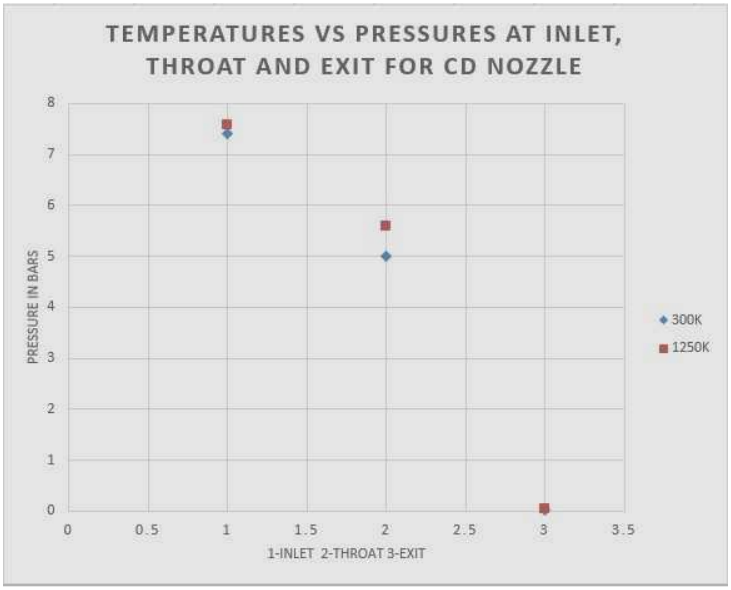

Figure 31: Variation of Pressure at Inlet, Throat and Exit of a CD Nozzle with Change in Inlet Temperature of the Fluid at 30 mbar Exit Pressure

From figure 31 it is observed that the inlet and exit pressures does not differ much in their magnitude but, the throat pressure is higher for the fluid with higher inlet fluid temperature.

Effect of Temperature on the Mach for Exit Pressure of 30mbar during Flow

The exit pressure of the fluid is taken as 30mbar with the inlet temperatures of 300K and 1250K. The contours are developed as shown in the figures Fig.5, and Fig.17. Variations of mach numbers with inlet temperatures are tabulated in table 15

Table 15: Mach numbers at Inlet, Throat and Exit at Different Inlet Temperatures at 30mbar

	Inlet Mach	Throat Mach	Exit Mach
At inlet temperature of 300K	0.0548	0.7076	4.228
At inlet temperature of 1250K	0.05523	0.69609	4.2236

The results are plotted on graph for understanding parametric effect shown in Fig.32

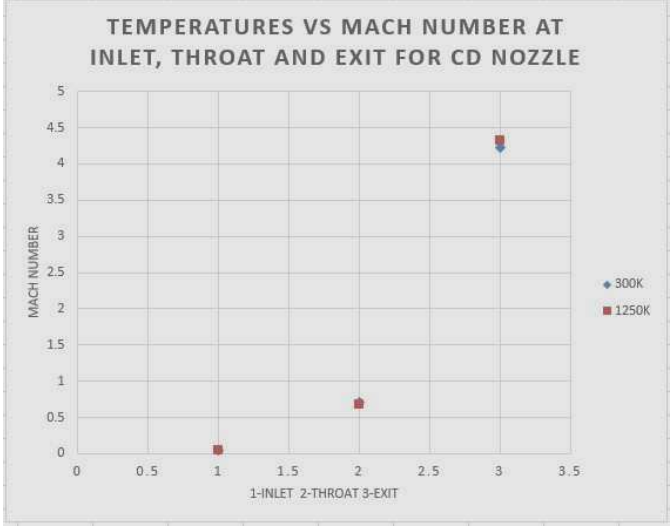

Figure 32: Variation of Mach number at Inlet, Throat and Exit of a CD Nozzle with Change in Inlet Fluid Temperature of the Fluid at 30 mbar Exit Pressure

From the figure 32 it is well observed that there is no appreciable change in mach number with raise in fluid inlet temperature.

Effect of Temperature on the Temperatures for Exit Pressure of 30mbar during Flow

The exit pressure of the fluid is taken as 30mbar with the inlet temperatures of 300K and 1250K. The contours are developed as shown in the figures Fig.9, and Fig.21. Variations of temperatures with inlet temperatures are tabulated in table 15

Table 16: Temperature at Inlet, Throat and Exit at Different Inlet Temperatures at 30mbar

	Inlet Temperature(K)	Throat Temperature(K)	Exit Temperature(K)
At inlet temperature of 300K	300	269.968	63.2
At inlet temperature of 1250K	1250	1145.35	263.811

The results are plotted on graph for understanding parametric effect shown in Fig.33. From figure 5.32 it is concluded that temperature of the inlet fluid reduces to a greater extent. The rate of decrease of temperature is directly proportional to the inlet fluid temperature.

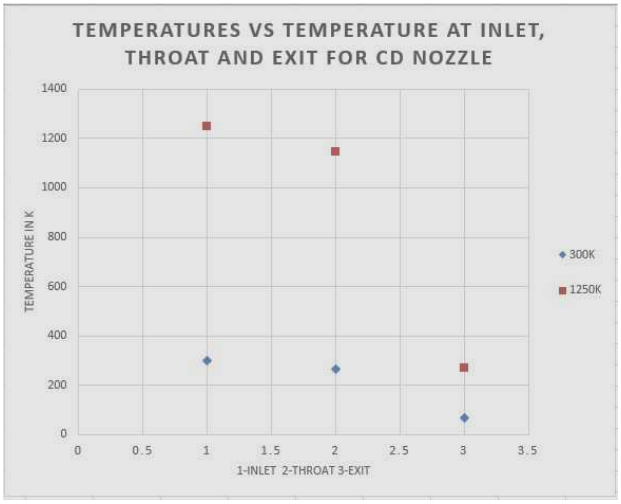

Figure 33: Variation of Temperature at Inlet, Throat and Exit of a CD Nozzle with Change in Inlet Fluid Temperature at 30 mbar Exit Pressure

CONCLUSIONS

This project is carried out with boundary conditions of inlet pressure 7.59bar, exit pressure 1050 mbar for CD nozzle. After performing flow analysis with ANSYS Cfx, the following conclusions are made.

- Pressure of fluid decreased and Mach is increased along the flow which facilitates the entrainment of low pressure exhaust gases with the high pressure motive air.
- Further no other fluid is used for the mixing of the fluids to increase the pressure of entrained exhaust gases to the ambient.
- Considerable decrease in the analysis time for convergence is also observed.
- Greater decrease in temperature of the inlet fluid is observed and the rate of decrease of temperature is directly proportional to the inlet fluid temperature. So, ejector system can be used in refrigeration systems namely Ejector Expansion Refrigeration System.

ACKNOWLEDGMENT

We extend our thanks to principal and management of Institute of Aeronautical Engineering for facilitating the softwares for the successful modeling and Analysis.

NOMENCLATURE

NAR	Nozzle Area Ratio	A_e	Exit area of cross section
CD	Convergent Divergent	A_*	Throat area of cross section
SED	Straight Cylindrical Exhaust Diffuser	P_t	Total pressure at inlet
STED	Second Throat supersonic Exhaust Diffuser	T_t	Total inlet temperature
NE	Nozzle Exit	$\dot{m}$	Mass flow rate
NPR	Nozzle Pressure Ratio	U_x	Momentum in X direction
ER	Entrainment Ratio	U_y	Momentum in Y direction
CR	Compression Ratio	U_z	Momentum in Z direction
u	Local flow velocity with respect to boundaries	P	Pressure
c	Speed of sound in medium	V	Velocity

V_e	Exit local velocity	h	Enthalpy
M_e	Exit mach number	β	Oblique shock angle
γ	Specific heat ratio	ρ	Density
R	Gas constant for exhaust gases	η	Efficiency
T_e	Exit Temperature		

REFERENCES

1. *Bogdan-Alexandru Belega, Trung Duc Nguyen, 2015, "Analysis Of Flow In Convergent-Divergent Rocket Engine Nozzle Using Computational Fluid Dynamics", International Conference Of Scientific Paper AFASES 2015 Brasov, pp. 28-30.*
2. *Prathibha, M. Satya Narayana Gupta, Simhachalam Naidu, 2015, "CFD Analysis on a Different Advanced Rocket Nozzles", IJEAT, 4(6), pp. 14-22, 2015.*
3. *Pardhasaradhi Natta, V. Rajah Kumar, Dr. Y. V. Hanumantha Rao, 2012 "Flow Analysis of Rocket Nozzle Using Computational Fluid Dynamics (CFD)", IJERA, 2(5), pp.1226-1235.*
4. *Balaji Krushna. P, P. SrinivasaRao, B. Balakrishna, 2013, "Analysis of Dual Bell Rocket Nozzle Using Computational Fluid Dynamics", IJRET, 2(11), pp. 412-417.*
5. *Shanthi Swaroopini, M. Ganesh Kumar, T. Naveen Kumar, 2015, "Numerical Simulation and Optimization Of High Performance Supersonic Nozzle At Different Conical Angles", IJRET, 4(9), pp. 268-273.*
6. *Omid Joneydi Shariatzadeh, Afshin Abrishamkar, and Aliakbar Joneidi Jafari, 2014, "Computational Modelling of a Typical Supersonic Converging-Diverging Nozzle and Validation by Real Measured Data".*
7. *G. Satyanarayana, Ch. Varun, S. S. Naidu, 2013, "CFD Analysis of Convergent-Divergent Nozzle", Acta Technica Corviniensis-Bulletin Of Engineering Tome VI – Fascicule 3.*
8. *CH. Srinivasa Chakravarthy1, R. Jyothu Naik, 2015, "Analysis Of Flow In A De Laval Nozzle Using Computational Fluid Dynamics", Proceedings of International Conference on Recent Trends in Mechanical Engineering-2K15(NECICRTME-2K15), pp. 2454-9614.*
9. *M. Sundararaj and S. Elangovan, 2013, "Computational Analysis of Mixing Characteristics of Jets from Rectangular Nozzle with Internal Grooves", Indian Journal of Science and Technology, 6(5S), pp. 4543-4548.*
10. *Saravanan Manikrishnan. P. Adhavan, C. Boobala Karthikeyan, Mohanraj Murugesan, and Sanal Kumar. V. R., 2014, "Numerical Studies on Altitude Compensation Nozzles for Aerospace Vehicles", 3rd International Conference on Mechanical, Automobile and Robotics Engineering (ICMAR'2014)*
11. *Syed Ashfaq, 2014, "Studies On Flow From Converging Nozzle And The Effect Of Nozzle Pressure Ratio For Area Ratio Of 6.25", IJESAT, 4(1), pp. 49-60.*
12. *Nadeem N, Dandotiya D, Najar F, 2013, "Modeling & Simulation of Flow Separation & Shocks in a CD Nozzle", IJMERA, 1(3), pp. 14-21.*
13. *Ms. B. Krishna Prafulla1, Dr. V. Chitti Babu and Sri P. Govinda Rao, 2013, "CFD Analysis of Convergent- Divergent Supersonic Nozzle", IJCER, 3(5), pp. 5-16.*
14. *Jean-Baptiste Mulumba Mbuyamba, 2013, "Calculation And Design Of Supersonic Nozzles For Cold Gas Dynamic Spraying Using Matlab And Ansys Fluent", Thesis, University of the Witwatersrand, Johannesburg.*
15. *Karla Keldani Quintão, 2012, "Design Optimization Of Nozzle Shapes For Maximum Uniformity Of Exit Flow", FIU Electronic Theses and Dissertations, Paper 779.*

16. *Ekanayake, E. M. Sudharshani, 2013, "Numerical Simulation of a Convergent Divergent Supersonic Nozzle Flow", Dissertation, RMIT University, Melbourne, Australia.*
17. *Srikrishna C. Srinivasa, 2012, "CFD Modeling and Analysis of an Arc-jet facility using ANSYS Fluent", Thesis, San José State University, San Jose, CA-95192.*
18. *Marc Linares, Alessandro Ciampitti Marco Robaina, 2015, "Design Optimization of Supersonic Nozzle", FIU.*
19. *CH V K N S N Moorthy , V Srinivas , V V S H Prasad and T Vanaja, 2017, "Computational Analysis Of A CD Nozzle With 'SED' For A Rocket Air Ejector In Space Applications", International Journal of Mechanical and Production Engineering Research and Development, 7(1), pp. 53-60.*
20. *CH V K N S N Moorthy, K Bharadwajan and V Srinivas, 2017, "Computational and Aero-Thermodynamic Design and Performance of Centrifugal Turbo-Machinery", International Journal of Mechanical Engineering and Technology, 8(5), pp. 320-333.*